CALIBRATION AND ARTEFACT MINIMIZATION IN A TWO WAVELENGTH CW DIFFUSE OPTICAL TOMOGRAPHY SYSTEM

Mihai PATACHIA[1]

In most of the tissues, light propagation is dominated by scattering. As result, after travelling the length of a few millimetres, light propagation in tissues can be described as a diffusive process. Different tissue types have distinct scattering properties, and therefore this distinction can be imaged. Using optical measurements at multiple source-detector positions on the tissue surface, one can reconstruct the internal distribution of the absorption coefficient (μa) and the reduced scattering coefficient (μ´s) based on the diffusion and the light transport model in a diffusive media. Measurements on phantoms are used to evaluate the performance of systems and to validate imaging algorithms. The calibration is the pivotal part of the data acquisition due to the variation in characteristics of each laser source, optical fibres, detectors and optic elements. An accurate calibration is achieved in homogeneous phantoms. The work describes how the homogeneous phantoms are used to evaluate the performance of the system and to minimize the artefacts.

Keywords: Laser diode, diffuse optical tomography, fibre optics, tissue phantom, image reconstruction.

1. Introduction

Started in 1929 as a simple transillumination, or diaphanography, the utilization of light to probe tissue has grew in the last years with the advent of new lasers, light detectors and fast computers and the development of the formalism for light propagation which demonstrates that light distribution in tissue can be well approximated with diffusion equation.

Diffuse optical tomography (DOT) is an optical technology that can be used to reconstruct spatial variations of optical properties in highly scattering optical media.

In the near-infrared (NIR) spectral window of 600 ÷ 1000 nm, photon propagation in tissues is dominated by scattering rather than absorption. Photons experience multiple scattering events as they propagate deeply into tissue (up to 10 cm) [1, 2].

[1]Department of Lasers, National Institute for Laser, Plasma and Radiation Physics, 409 Atomistilor St., PO Box MG-36, 077125 Magurele, Ilfov, Romania, mihai.patachia@inflpr.ro

In the diffuse optical tomography, the optical properties of the translucent soft tissue are reconstructed based on measurements of near-infrared light on the boundary of the object. To obtain such data, the diffuse optical tomography uses movable light sources and detectors attached to the surface of the target media. There are three main measurement schemes, namely: FD (frequency domain), TD (time domain) and CW (continuous-wave) [3-8].

Because CW method is more accessible from the technical point of view (low frequency modulation, high sensitive detectors, etc.), being at the same time the simplest and least expensive from the three schemes, we have used this measurement scheme in the construction of our DOT laboratory model.

2. Experimental setup

Our experimental setup is an automated multi-channel CW system that uses an overlaid intensity-modulated light from two laser diodes (785 nm – 1 W and 830 nm - 500 mW, Roithner Lasertechnik), sequentially sent to the target media through eight 3-mm fibre optic bundles. The two beams of the laser diodes are coupled together by a fibre optic coupler (RoMack Inc.) and two collimators (C230220P-B, ThorLabs Inc.). For each source position, the diffused light is received at 8 detector locations along the surface of the cylindrical measuring head. The serial approach for illumination and detection is achieved with one optical demultiplexer and one optical multiplexer controlled by two translation stages (PI M505.2S2, Mercury Inc.).

The two translation stages use microprocessor-controlled stepper motors (20,000 counts/rev.) that provide ultra-smooth, vibration free, 0.1 μm minimum incremental motion steps and allow a relatively fast and precise positioning of the fibres over a 50 mm travel range. Fig. 1 shows the source / detector arrangement in the measuring head (optode).

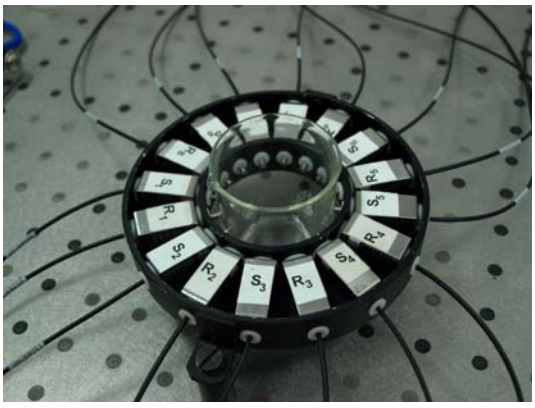

Fig.1 The measuring head of the CW DOT laboratory model

For each experimental configuration, a total of 128 measurements are made in less than 60 seconds using a variable-gain photodetector OE-200-SI (FEMTO Messtechnik GmbH) equipped with 1.2 mm active diameter Si photodiode, two lock-in amplifiers LIA-MV-150 (FEMTO Messtechnik GmbH) and a 12 bit A/D acquisition board (KUSB3102, Keythley Instr. Inc.).

System operation is achieved by three levels of software control. The first level is responsible for system timing, the second for data storage and the third for image reconstruction based on μa and μ′s coefficients distributions. The user interface in the first level is realized under MMCRun for Mercury and the collected data are made available in four registration channels, two for the intensity measured at the boundary of the tissue and two for the TTL signal generated by the translation stages during the motion, to provide the data viewing and analysis in real time for secondary level within a Keithley QuickDAQ environment.

The third software used in the system enables the reconstruction algorithm. The reconstruction algorithm uses a regularized Newton's method to update iteratively an initial optical property distribution, in order to minimize an object function composed of a weighted sum of the squared difference between computed and measured optical data at the tissue surface. The computed optical data (i.e., photon density) is obtained by solving the photon diffusion equation with finite element method.

For the measuring head with 8 illumination fibres and 8 receiving fibres we have used a mesh with 368 elements (voxels) and 217 nodes.

3. System calibration

Optical fibers are used both to conduct light from the sources to the tissue and to transfer the collected light from tissue to detectors. An adaptive interface was constructed to hold the sample and position the tips of source and detector fibers around the full circumference of the sample. It consists of eight-source and eight detector fiber probes with radially adjustable holders (Fig. 2).

A compression spring is used for each probe to provide the required pressure to hold the fiber on the sample surface. The design allows to have the same pressure level at each probe position. The sample is placed at the center of the fiber optic interface, and the fiber probes are radially adjusted until they are in contact with the sample.

Measurement repeatability is also an important factor that affects the performance of the imaging system. To separate the errors arising from the fiber positioning and the instrument itself, repeatability tests were conducted with and without the repositioning of the homogeneous phantom.

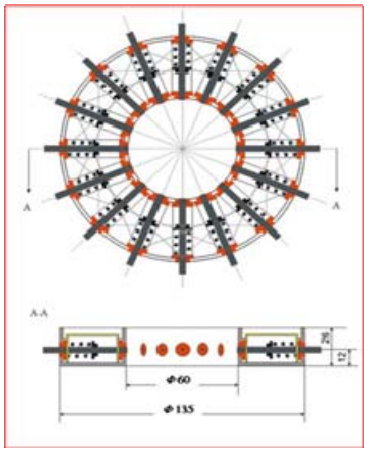

Fig. 2 Interface adapted to maintain sources and detectors at sample circumference

To eliminate the errors due to the inhomogeneity of the phantom, it was placed in the same orientation each time it was repositioned. In this case, the average rms error in the amplitude measurements were found to be about 5%. This error was caused only by the fiber probe repositioning.

Later, the phantom was also rotated 45 deg between each measurement and the same error values were obtained. Therefore, it was concluded that the error due to the spatial variations of the phantom optical properties is less than the fiber repositioning errors. At the end of each experiment, a homogeneous phantom is placed in the fiber optic interface to acquire calibration data. The errors due to fiber repositioning would result in errors in the calibration and therefore affect the reconstructed image quality. These errors would cause fluctuations in the recovered optical properties in the imaging volume close to the source and detector probes, in addition to the inaccuracy in the recovered optical properties of the inclusion.

For the mathematical representation of the light transport in the measuring media, it is convenient to divide the calibration problem into three components, i.e., factors associated with the source fibre, with the target medium, and with the detecting fibre [9], while the following initial conditions are supposed to be fulfilled:

- all source intensities and detector efficiencies are time invariant;
- each detector reading is a measure of light that has entered a target medium at only a single location (i.e. the light which is detected was exited from only a single location).

The transfer function can be expressed in this case as a matrix equation:

$$R = c\, Pl S M D$$

where the elements in R are the detector readings rnj, S and D are diagonal matrices whose elements represent the composite loss factors dj and sn, respectively; and the elements in matrix M are the mnj values attributable to losses occurring in the medium; c is the detector sensitivity and Pl is the laser power. The goal of calibration is to determine the entries of D and S, given the set of measured values in R.

The first step in the DOT calibration is the evaluation of the light transfer coefficients through optical fibres used as illuminations sources and light receivers on the measuring head.

For precise measurement of the power in the input and the output of the optic fibres used for illumination and detection, we have used a laser radiometer Vega (Ophir) equipped with an integrating sphere model 3A-IS-IRG as measuring head, which has a resolution of 1 nW for a maximum power of 1W and it's calibrated with 1 nm step in the near infrared range.

The calibration curve for the detection fibres and illumination fibres are presented in Figs 2 and 3 respectively.

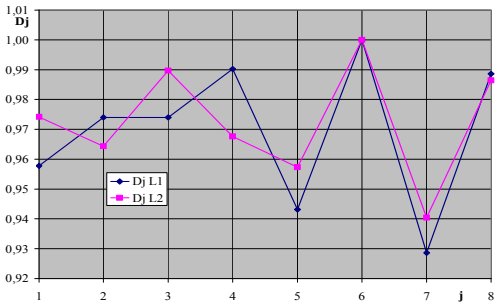

Fig. 3 Detector coupling efficiency D*j* versus detector number *j* for the two laser wavelengths L_1 and L_2

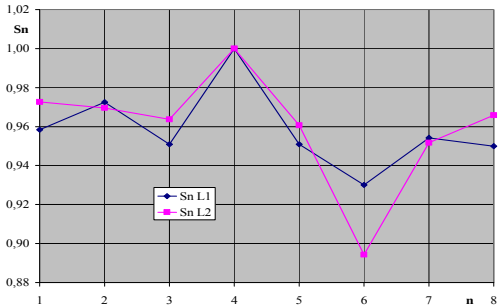

Fig. 4 Illumination coupling efficiency S*n* versus source number *n* for the two laser wavelengths L_1 and L_2

The elements rnj of the matrix R are the light intensity values used in the characterization of the optical properties of the target media (tissue phantom) and they can be find either directly from the transfer equation (1) using the iterative proportional fitting (IPF) technique [10], or solving the forward problem for a finite-element model [11].

4. Artefact minimization in the reconstruction process

To put in evidence the selective absorption of the hemoglobin at 785 nm we investigated a liquid phantom made with 1% Lipofundin in a 50 mm diameter glass recipient and two thin 4 mm diameter glass tubes filled with diluted bovine hemoglobin (Fig. 5).

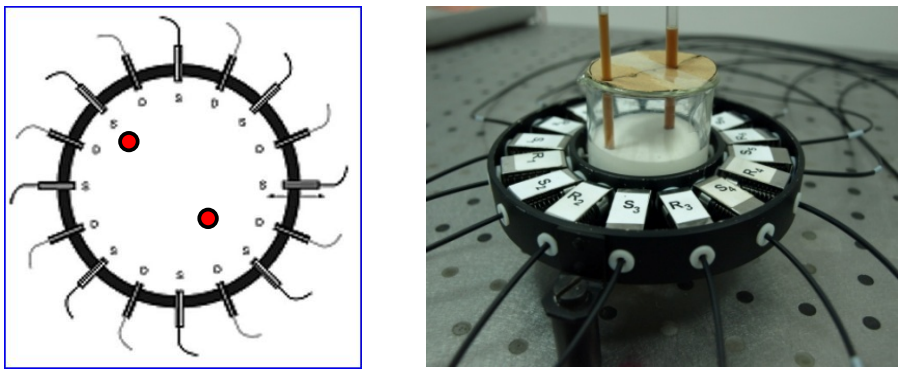

Fig. 5 The cross section in the measuring plane and the liquid phantom made with 1% Lipofundin in a 50 mm diameter glass recipient and two thin 4 mm diameter glass tubes

In Fig. 6 the mesh used in the reconstruction program (368 elements (voxels) and 217 nodes) and the resulting XY distribution of the μa and μ′s coefficients computed with the 128 measured data at the boundary of the probe are presented.

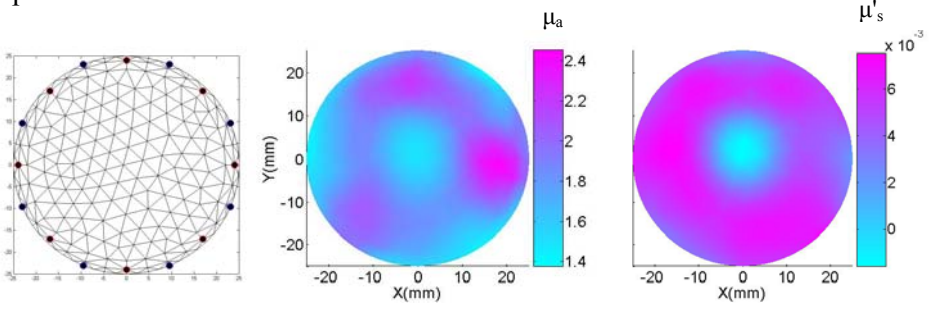

Fig. 6 The mesh structure and the XY distribution of the μ_a and μ'_s

In the case of the phantom with diluted bovine hemoglobin, the intensities detected at the boundary are smaller for the wavelength of 785 nm due to the selective absorption of the solution at this wavelength in comparison with the 1% intralipid solution, where this selectivity is not present.

The result shows many artefacts in the reconstructed distribution and a deviation of the two tubes cross section from the diameter of the probe. The causes of this situation are the glass walls of the recipient and of the two tubes. To minimize the influence of the glass walls in the measurement results, we have used a differential method which compares the XY distributions of μa and μ′s in 1% Lipofundin without and with the inhomogeneity induced by the presence of the tubes filled with hemoglobin.

The new XY distributions obtained by this method are presented in Fig. 7. One can easily observe a decrease of the artefacts number in the probe reconstructed image and a more precise location of the two tubes in the phantom geometry.

Systematic errors in optical signal detection need to be eliminated by careful normalization of the data or optimizing the contact with the probe by replacing glass recipient with a plastic recipient with a window sealed with latex thin film in front of each optical fiber (Figure 8).

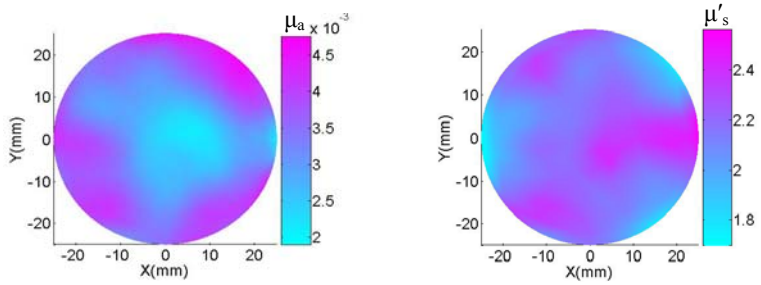

Fig. 7 The XY distribution of the μ_a and μ'_s after compensation with the measured distribution for 1% Lipofundin in glass recipient

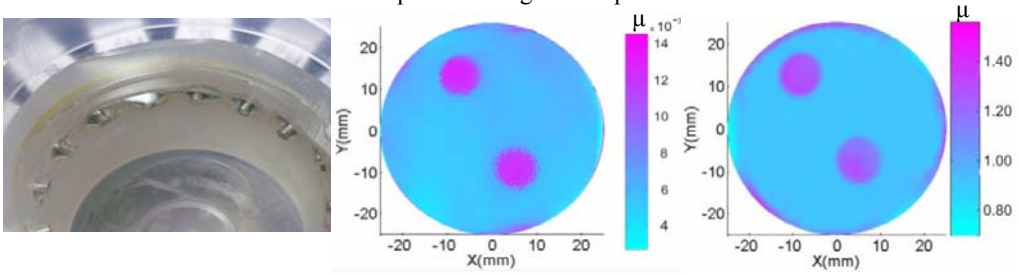

Fig. 8 The XY distribution of the μ_a and μ'_s after compensation with the measured distribution for 1% Lipofundin in plastic recipient with a window sealed with latex thin film in front of each optical fiber.

In this multiple source-detector arrangement, variations in transmitted intensity among different fibers ranged up to 10%. This level of systematic intensity variation must be corrected in the measurements before the data can be used in the reconstruction algorithm. In the cases presented here, the heterogeneous phantom image data was normalized by data collected from a homogenous phantom. At this point, it is still not clear whether the limiting noise in the system will be systematic or statistical, although this depends upon the signal from each source-detector pair. At detector locations near the source, systematic error tends to impose the limitation on precision, while at detectors far from the source, where there is not much light signal, statistical errors from the detector dominate. In spite of these limitations, accurate absorption coefficient images can be created with the system for imaging phantoms which are similar to breast tissue. The reconstruction of the absorbing object is quantitatively correct and the method is encouraging for images based upon changes in absorption. The second image of a diffusing object (Fig. 7) does not reconstruct properly, because there is a slight artifactual reconstruction of the diffusing effect into the absorption coefficient image (i.e. the presence of a pure absorbing and diffusing inhomogeneity cannot be exactly separated with the measurements obtained by this instrument. These results suggest that measurements are better when can discriminate between absorption and scattering, such as the use of higher frequency modulation.

5. Conclusions

To increase the reconstruction precision in the CW Diffuse Optical Tomography of turbid media, it's important either to increase the number of the measuring data by enlarging the number of the wavelengths used to illuminate the target, or to increase the number of the illuminating and measuring fibres. The increase in resolution needs the development of computation algorithms able to eliminate the influence of wall barriers and the imperfect contact between the optical fibres and the tissue.

The correct use of the CW method needs however a special effort to solve the non-uniqueness problem of the method which lacks the capability to separate absorption from scattering in the Optical Tomography- OT image reconstruction. For this aim the CW imaging needs preconditioning and regularization techniques and multispectral laser sources.

In conclusion, we can highlight the following aspects:

- Diffuse optical tomography (DOT) can image spatial variations in highly scattering optical media;
- The error due to the spatial variations of the phantom optical properties is less than the fiber repositioning errors;

- The multifrequency approach reported in this manuscript has great potential to substantially increase the quality of the images obtained by diffuse optical tomography systems;
- The use of thin latex membrane at the measuring boundary of the probe avoids the strong reflections and diffusion at the walls of the recipient.
- The technique developed as part of this research may also aid the development of new industrial applications where imaging through strongly scattering media is required.
- The measurement procedure is non-invasive and the radiation is non-ionizing, and therefore the technique is patient safe.

Acknowledgements

Thank you to Prof. Dr. H. Jiang and Mrs. Xiaoping Liang from the Department of Biomedical Engineering, University of Florida, Gainesville, U.S.A. and Dr. N.V. Iftimia, Physical Sciences, Inc., 20 New England Business Center Drive, Andover, U.S.A.

R E F E R E N C E S

[1]. *J. R. Mourant, T. Fuselier, J. Boyer, T. M. Johnson, and I. J. Bigio*, Predictions and measurements of scattering and absorption over broad wavelength ranges in tissue phantoms. Appl.Opt. 39, 949–957 (1997).

[2]. *M. K. Nilsson, C. Sturesson, D. L. Liu, and S. Andersson-Engels*, Changes in spectral shape of tissue optical properties in conjunction with laser-induced thermotherapy. Appl.Opt. 37(7), 1256–1267 (1998).

[3]. *H. Jiang, Y. Xu, N. Ifitimia, J. Eggert, K. Klove, L. Baron, and L. Fajardo*, Three dimensional optical tomography imaging of breast in a human subject. IEEE Trans. Med. Imaging 20, 1334–1340 (2001).

[4]. *N. Iftimia, X. J. Gu, Y. Xu, and H. B. Jiang*, „ A compact, parallel-detection diffuse optical mammography system" Rev. Sci. Instrum. 74, 2836-2842 (2003).

[5]. *B. W. Pogue, S. P. Poplack, T. O. McBride, W. A. Wells, K. S. Osterman, U. L. Osterberg, and K. D. Paulsen*. Quantitative hemoglobin tomography with diffuse near-infrared spectroscopy: Pilot results in the breast. Radiology 218, 261–266 (2001).

[6]. *B. W. Pogue, S. D. Poplack, T. O. McBride, S. Jiang, U. L. Osterberg, and K. D. Paulsen*. Breast tissue and tumour haemoglobin and oxygen saturation imaging with multi-spectral nearinfrared computed tomography, In Adv. Exp. Med. Biol. International Society on Oxygen Transport to Tissue Plenum Press Aug. (2001).

[7]. *H.Wang, M. E. Putt, M. J. Emanuele, D. B. Shin, E. Glatstein, A. G. Yodh, and T. M. Busch,* Treatment-induced changes in tumor oxygenation predict photodynamic therapy outcome, Cancer Res. 64, 7553–7561 (2004).

[8]. *R. Choe, A. Corlu, K. Lee, T. Durduran, S. D. Konecky, M. Grosicka-Koptyra, S. R. Arridge, B. J. Czerniecki, D. L. Fraker, A. DeMichele, B. Chance, M. A. Rosen, and A. G. Yodh*, „Diffuse optical tomography of breast cancer during neoadjuvant chemotherapy: a case study with comparison to MRI", Med. Phys. 32(4), 1128-1139 (2005).

[9]. *C. H. Schmitz, H. L.Graber, H. Luo, I. Arif, J. Hira, Y. Pei, A. Bluestone, S. Zhong, R. Andronica, I. Soller, N. Ramirez, S. Barbour, and R. L. Barbour*, „Instrumentation and calibration protocol for imaging dynamic features in dense-scattering media by optical tomography", Applied Optics 39, 6466-6485 (2000).

[10]. *Y. M. M. Bishop, S. E. Fienberg, and P. W. Holland*, "Maximum likelihood estimates for complete tables," in Discrete Multivariate Analysis: Theory and Practice MIT, Cambridge, Mass., (1991), Chap. 3.

[11]. *H. B. Jiang, Y. Xu, and N. Iftimia*, „Experimental three-dimensional optical image reconstruction of heterogeneous turbid media from continuous-wave data", Optics Express 7, 204-209 (2000).